6.1 Introduction

Organic arsenic, a less toxic form of arsenic present in the form of roxarsone (ROX) (3-nitro-4-hydroxyphenyl arsonic acid) as an enhanced animal drug used for the treatment of parasitic disease coccidiosis, could be converted into inorganic arsenic [382,383]. It is also injected into the chicken that is bred specifically for meat consumption in poultry farming [383,385]. Chickens that consumed roxarsone-containing feed (20−40 mg kg^{-1}) demonstrated arsenic concentrations of 3−7, 2−5, and 2−6 μg kg^{-1} in the liver, muscle, and heart, respectively [386]. Many of the arsenic compounds released from animal waste are water soluble, thereby increasing inorganic arsenic in the environment and causing contamination. Acceptable levels of arsenic in different countries range from 50 to <10 ppb in drinking water. In addition, the consumption of roxarsone in meat must be 5.0−6.0 mg Kg^{-1}. Higher concentrations of arsenic are closely related to serious cancer toxicity in humans[387-389]. Long-term arsenic exposure also implies cardiovascular diseases [390], neurological disorders [391], diabetes [392], birth-related issues [393], and endocrine disorders [394]. Therefore, a profound diagnosis of roxarsone has attracted increasing attention from researchers in food analysis and human health-oriented platforms.Electrochemical methods are widely used in the detection of several feed additives, as they have low costs, good sensitivity and selectivity, and rapid detection and portability [395-399]. However, there are a few reports in which electrochemical sensing is performed for the detection of ROX [400-402].Carbon-based materials have attracted immense attention as electrode materials because of their high electrical conductivity, specific microstructure, and good stability. Such carbon materials can be engineered for good sensitivity and selectivity [403,404]. Apart from several graphene or CNT-like materials, it is also important to explore environment-friendly, efficient, and cost-effective carbon materials for several applications. Toward this end, biomass-derived activated carbon materials have been attracting competent interest due to their high surface area, less toxicity, adjustable pore size, good electrical conductivity, chemical stability, and the presence of heteroatoms that provide good functionality [405-407].Activated carbon is a carbon-containing solid that is obtained from biomass, biochar, coal, lignite, and petroleum pitch, using pyrolysis. In the process, a carbon material is processed for increased surface area, allowing it to absorb a larger quantity of molecules and chemical reactions. The large surface area of

activated carbons results in a greater amount of porosity. The activation can be performed by either physical or chemical activation processes. In physical activation, the precursor is pyrolyzed in the 600−1200 °C range in an inert atmosphere, and the obtained carbonized product is activated by CO_2 [408]and steam [409]. While in chemical activation, alkali and metal salts such as $MgCl_2$ [410], K_2CO_3 [411], KOH [412], Na_2CO_3 [413], NaOH [414], $ZnCl_2$ [415] and H_3PO_4 [416] are used along with precursors, and the obtained product is pyrolyzed in the 400−950 °C range. The synthesis of activated carbon is simple, environment-friendly, and economical. Very recently, eragrostis cynosuroids (grass family) were used as a source of activated carbon for energy storage devices using $ZnCl_2$ as an activating agent [417] Activated carbons have been used in several applications such as Li-ion batteries [418], sensors [419], super-capacitors [420], removal of toxic metal ions and organic dyes[421], and electrocatalysts [422]; however, their application in electrochemical sensing is not extensive. In the present study, meso/microporous activated carbon (2D carbon) was prepared from natural biomass Kusha grass (Desmostachya bipinnata) using KOH as an activating agent, which enhances further the adsorption capacity of the exposed surface for metal adsorption. Desmostachya bipinnata belongs to the grass family, Poaceae. The motivation behind choosing Kusha grass was that the rate of production of such agricultural waste including grass, leaves, and flowers is very high in India. These materials have high lignin and cellulose contents containing carboxylic and phenolic polar functional groups, which also have a metal-binding ability [423,424]. The present study provides a first-of-its-kind allocation with the fabrication of highly electroactive surface areas for electrode modification using bio waste. Till now, no literature reports have been available for the sensing of toxic drug ROX on this biowaste-derived activated carbon (2D carbon) for the modification of commercial electrodes using the differential pulse voltammetry (DPV) method. Hence, we deal with such abundant biomass-derived activated carbon, which has no toxicity, is environment-friendly, and provides an economical alternative option as a new electrode material for electrochemical sensing. However, earlier reports available for the electrochemical sensing of ROX have used hazardous toxic chemicals for electrode material preparation.

6.2 Results and Discussion

6.2.1 Characterization of Activated Carbon

The X-ray diffraction (XRD) pattern of the prepared 2D carbon in Fig.6.1(a) shows two characteristic peaks of any activated carbon. Peaks at 22° and 43.5° correspond to (002) and (101) planes, respectively. The (002) peak is broad at the base and sharp at the top containing both the amorphous and crystalline nature of graphitic carbon and indicating the presence of a few single exfoliated layers [425]. The peak at 43.5° is ascribed to the creation of pores due to the decomposition of the carbon ring in the direction of the graphitic arrangement and the formation of more organized aromatic carbon. Such a newly formed structure was more stable than the amorphous carbon only. Raman spectra after carbonization and activation are shown in Fig. 6.1(b). The two strong peaks displayed in the spectra correspond to the D-band and G-band, respectively. Inactivated carbon, the G-band is broad and occurs at 1580 cm^{-1}, relating to the first-order Raman band of the sp^2-bonded graphitic region. Also, the peak at 1345 cm^{-1}, which corresponds to the D-band, occurs because of amorphous carbon (disordered), grain boundaries, and size reduction of the sp^2-bonded carbon network [426]. The intensity ratio of the D and G bands is used to determine the degree of sp^2 ordering in carbon materials. It is found that after activation, the I_D/I_G value representing the disorderliness is considerably more than that of the carbonized sample (from 0.83 to 0.96), signifying that the activation process allowed for activated carbon (AC) to have more defective sites upon thermal reduction [427]. Kusha grass contains a high content of organic components such as lignin and cellulose and various types of polar functional groups such as phenolic and carboxylic acids. The FTIR spectrum shown in Fig. 6.1(c)depicts a broad absorption peak at around 3150 cm^{-1}, which may be due to the presence of intermolecular hydrogen bonding in hydroxyl, O−H in phenolic, carboxylic, and alcoholic groups. The small peak at 2930 cm^{-1} is attributed to the C−H stretching in CH, CH_2, and CH_3 groups. The peak at 2350 cm^{-1} C=O stretching in CO_2, which may be adsorbed on surface activated carbon. The prominent band at 1630 cm^{-1} occurs due to the C=O stretching in carbonyl groups. The peaks at around 1450 and 1355 cm^{-1} are due to the O−H bending vibration and 1130−1060 cm^{-1} is due to the C−O stretching vibration. While the peaks from 630 to 1000 cm^{-1} can be attributed to C−H deformation in alkynes, C−H bending (out of plane) in alkenes, C−H bending and ring crumpling in

arenes, O−H bending (out of plane), and C−X stretching of halo compounds [428]. The surface morphology of as-prepared 2D carbon was first investigated using scanning electron microscopy, as shown in Fig.6.1(d). Foam or spongelike defects on the surface having several pores of different sizes can be observed. It also describes that such irregularities were developed during the activation process. The bigger size was probably due to sample preparation, where the powder form of AC was taken, which becomes agglomerated. Further, transmission electron microscopy was also performed to observe the structure of the prepared sample. Fig.6.1(e) shows the interconnected pores formed inside the 2D carbon sheets. This may be due to the evolution of gases during carbonization. The dispersed sample was used in this characterization, where the nanometer-sized material formation was justified. The porosity nature of as-synthesized activated carbon was examined using N_2 adsorption−desorption isotherms, as shown in Fig. 6.1(f). The figure shows type IV nitrogen adsorption isotherms where the black line shows N_2 adsorption while the red line represents its desorption. The red line did not follow the path of the black line and formed a loop-like structure between 0.45 and 0.95 relative pressures (P/P_0). Such features advocated the occurrence of micro- and mesopores in the sample. The creation of this loop indicates that 100% N_2 was not released and was trapped in the small pores present in the AC. The inset of this figure shows the corresponding pore size distributions obtained from the Barrett−Joiner−Halenda (BJH) method, which also emphasized the presence of micro- and mesopores (0.4−2.8 nm), where the average pore diameter was found to be 1.79 nm. The specific surface area of the as-synthesized AC was found to be 194 m^2 g^{-1}. The presence of such a small pore diameter offered a good corridor for strong adsorption of the target analyte and further led to enhanced electrochemical performance and high sensitivity of 2D carbon as suitable electrode material for sensing [429,430].

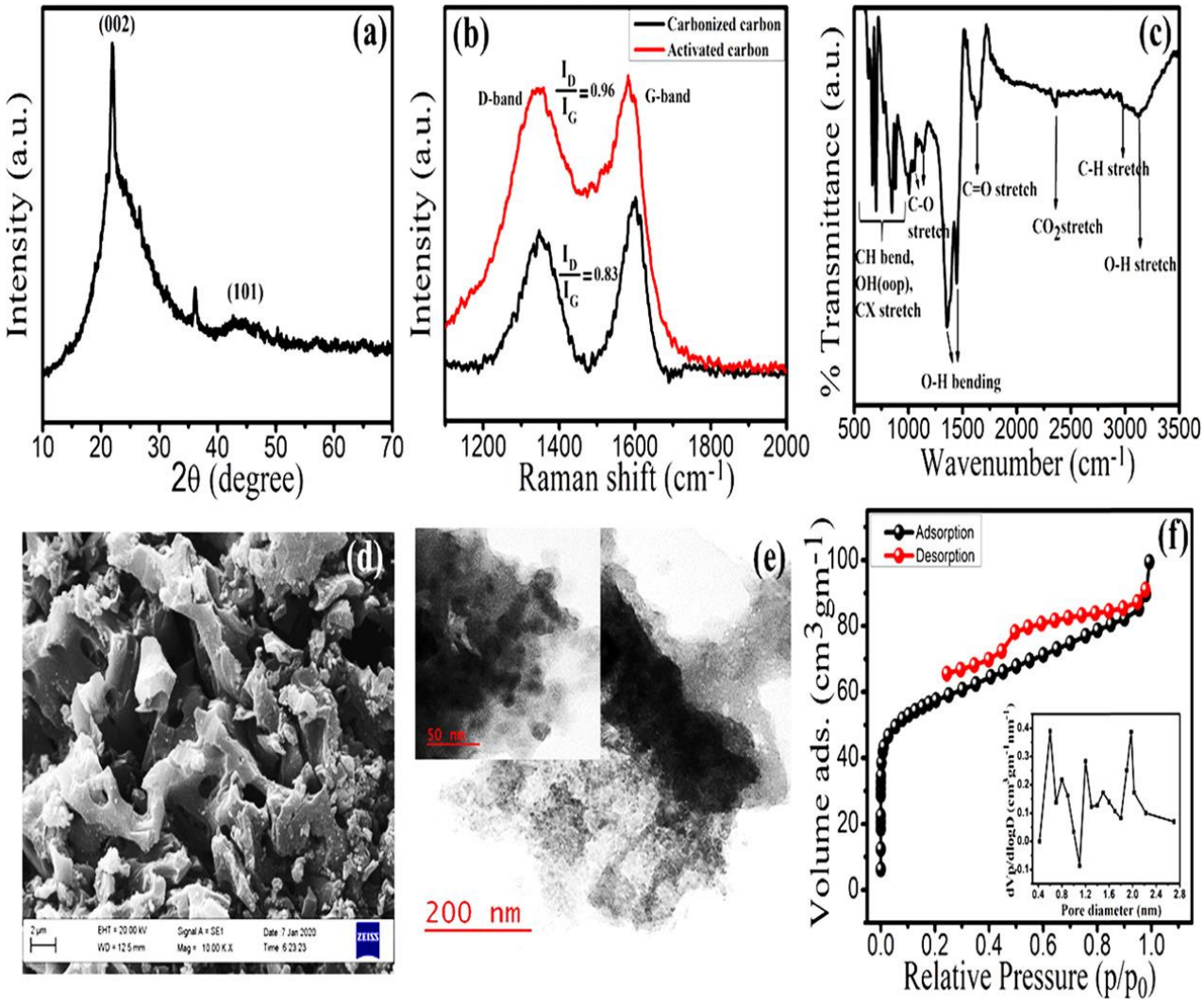

Fig. 6.1 Characterization of two-dimensional (2D) activated carbon using (a) XRD, (b) Raman (before and after activation) (c) Fourier transform infrared (FTIR) spectroscopies, (d) scanning electron microscopy (SEM), and (e) high-resolution transmission electron microscopy (HR-TEM) image; the inset shows an enlarged view of the TEM image. (f)N_2 adsorption−desorption isotherms; the inset shows the pore size distribution curve.

6.2.2 Electrochemical Studies

6.2.2.1 Effect of pH and a Comparative Study of Differently Modified Electrodes

A glassy carbon electrode was chosen and modified with the prepared activated carbon for this particular study; then, the electrochemical performance of ROX at the AC-modified glassy carbon electrode (GCE) was investigated using DPV with pH values of 5, 6, 7, and 8 for obtaining optimal conditions to obtain high peak currents and well-defined peak shapes. The results are shown in Fig.6.2(a). It can be seen that the cathodic peak current increases from 5 to 7 and thereafter decreases. Also, the peak potential shifts to a more negative value from pH 5 to 8. Additionally, pH 7.0 is more stable and shows a better response; therefore, we can choose a phosphate-buffered saline (PBS) solution of pH 7.0 for subsequent electrochemical experiments [401]. Furthermore, the electrochemical behaviour of bare and AC-modified GCE was studied in potassium ferrocyanide/ potassium ferricyanide (Fe(II)/Fe(III)) redox couple. Results obtained are shown in Fig. 6.2(b), where peaks of 2D carbon-modified GCE were shifted toward lower potential as compared to bare GCE in the presence of the redox probe $K_3[Fe(CN)_6]/K_4[Fe(CN)_6]$ in 0.1 M PBS with current enhancement, which was attributed to the rapid electron transfer kinetics with a superior electroactive surface area of the modified electrode. This shifting of potential indicated the catalytic behaviour of the prepared material. The electrochemical behaviour of the prepared 2D carbon was also determined in 0.1 M PBS only (pH 7) with and without ROX at both bare and modified GCE, as shown in Fig.6.3(c). The figure depicts that the addition of 76 μM ROX over bare GCE did not show a clear change, while 2D carbon-modified GCE gave a significant reduction peak at 0.66 V in DPV. Also, the efficiency of synthesized AC is compared and validated on commercially available graphite powder (Gr)-modified GCE with and without ROX. It was also evident from Fig.6.2(c)that the Gr-modified GCE did not give a well-resolved peak with our analyte roxarsone. Such superior nature of as-synthesized 2D-AC may be because of its big porous structure bestowing a large surface area, excellent conductivity, and rapid mass and electron transfer. In all cases, the signature was observed almost at the same potential. To validate the effect of surface area, the electrochemical active surface area (EAS) was calculated using the Randles−Sevick equation [431] by cyclic voltammetry technique in 5.0 mM

$K_3Fe(CN)_6/K_4Fe(CN)_6$ as a test solution in 0.1 M PBS buffer, at different sweep rates and T = 298 K for bare GCE, Gr-modified GCE, and AC modified GCE as follows

$$Ip = 2.69 \times 10^5 A D^{1/2} n^{3/2} v^{1/2} C \quad (6.1)$$

where A is the area of the electrode surface, D is the diffusion coefficient, i.e., 7.6×10^{-6} cm^2 s^{-1}, ν is the sweep rate (mV s^{-1}), and C is the concentration of $K_3Fe(CN)_6$ /$K_4Fe(CN)_6$ redox couple in the electrolyte. From the slope of the plot of Ip vs $v^{1/2}$, the approximate value of the surface area of the bare GC electrode, graphite-modified GCE, and AC-modified GCE was found to be 0.052, 0.065, and 0.075cm^2, respectively. The above findings lead us to perform a comparison of charge transfer behaviour between the reference electrode (RE)and the vicinity of bare and modified electrodes (usually called a working electrode, WE) using electrochemical impedance spectroscopy (EIS). EIS was performed at their open-circuit potentials (OCPs) within a frequency range from 0.01 Hz to 100 kHz with an AC amplitude of 5 mV at room temperature. EIS analysis shows the behaviour of the glassy carbon (GC) electrode surface and determines the interfacial properties of 2D carbon over it. Fig. 6.2(d) shows the Nyquist plot of the bare and modified GCEs with and without 76 μM drug in 0.1M PBS buffer solution at pH 7. The inset shows the zoomed-in part of the same Nyquist plot. A general explanation of the EIS plot depicts that if the formation of the semicircle is inclined to the Z'-axis and/or linked with a straight line at about a 45°angle, then it is said to be the outcome of resistance to charge transfer between working and reference electrodes with diffusion-dominated mass transfer in the surrounding area of the working electrode [432]. Similarly, it is also reported and demonstrated in the literature that the inclination of the straight line toward the Z'-axis expresses more charge accumulation on the working electrode as compared to its counter ones [433]. From Fig. 6.2(d) curves "ii" and "iii" are more inclined toward the Z'- axis as compared to curve "i" showing more charge accumulation on the electrode surface and favouring a diffusion-dominated phenomenon. However, on comparing curves "ii" and "iii", it was observed that after the addition of 76 μM ROX, curve "iii" was inclined toward the Z'-axis, creating more resistance as some active sites on the modified electrode were now covered by the analyte moiety. Hence, 2D carbon shows efficient electrical communication at the electrode surface.

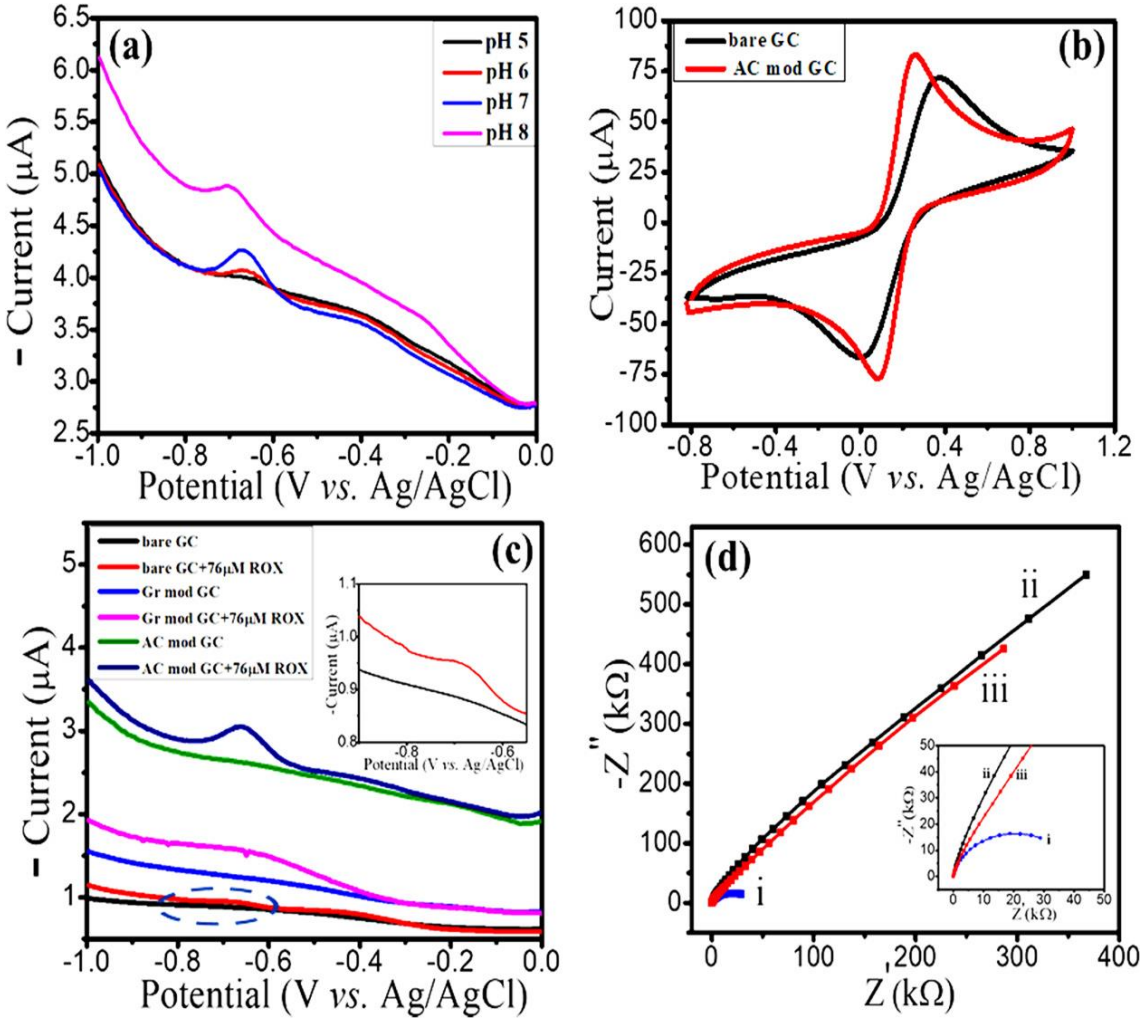

Fig. 6.2 (a) Study of different pH values using DPV; (b) CV plot of bare and 2D-AC-modified GCE in 5.0 mM $K_3[Fe(CN)_6]/K_4[Fe(CN)_6]$ redox couple in 0.1 M PBS at the scan rate of 50 mV s^{-1}; (c) DPV plot of bare GCE, graphite powder (Gr)-modified GCE, and 2D-AC-modified GCE in 0.1 M PBS at pH 7 in the absence and presence of 76 µM ROX (the inset shows an enlarged view of the dotted circled area); and (d) the Nyquist plots of (i) bare GCE, (ii) 2D-AC without ROX, and (iii) 2D-AC-modified GCE with 76 µM ROX.

6.2.2.2 Electrocatalytic Reduction of Roxarsone over GCE

Differential pulse voltammetry was applied to discuss the catalytic nature of 2D carbon-modified GCE for different concentrations of the toxic drug ROX. In Fig. 6.3(a), ROX showed a reduction peak at −0.66 V. The entire study was performed in the −0.4 to −1.0 V potential range, and the study was conducted in a linear range of 0.76−474 μM (there was saturation beyond 474 μM, observed at 549.62 μM). From the figure, it is evident that the cathodic peak or reduction peak for ROX increases excellently with an increasing concentration of ROX at 2D carbon-modified GCE. 2D carbon permitted better electron transfer on the surface of GCE and showed an extremely good linear response toward ROX, as shown in Fig.6.3(b). The experiment was carried out in triplicate. However, error bars were added by calculating current variations in each set of experiments at a fixed concentration of ROX. This nonenzymatic electrochemical sensor exhibits a good sensitivity of 0.0714 $\mu A \cdot \mu M^{-1} \cdot cm^{-2}$ with $R^2 = 0.997$. Then, the limit of detection (LOD) was measured by back extrapolation of the linear fit line on the Y-axis and calculated to be 1.5 nM, whereas the LOQ (limit of quantification) was 0.76 μM. Table 6.1 shows the comparative analytical performance toward

ROX with a few previously reported research articles. However, we found that very few reports in the literature were related to the electrochemical method. Additionally, the proposed electrochemical reaction mechanism is shown in Fig.6.4, describing the reduction of ROX in the presence of 2D carbon-modified GCE. It demonstrates the electroreduction of NO_2 to NH−OH, which occurs at −0.66 V and undergoes an irreversible reduction process as there is no anodic peak observed in CV [400,401].

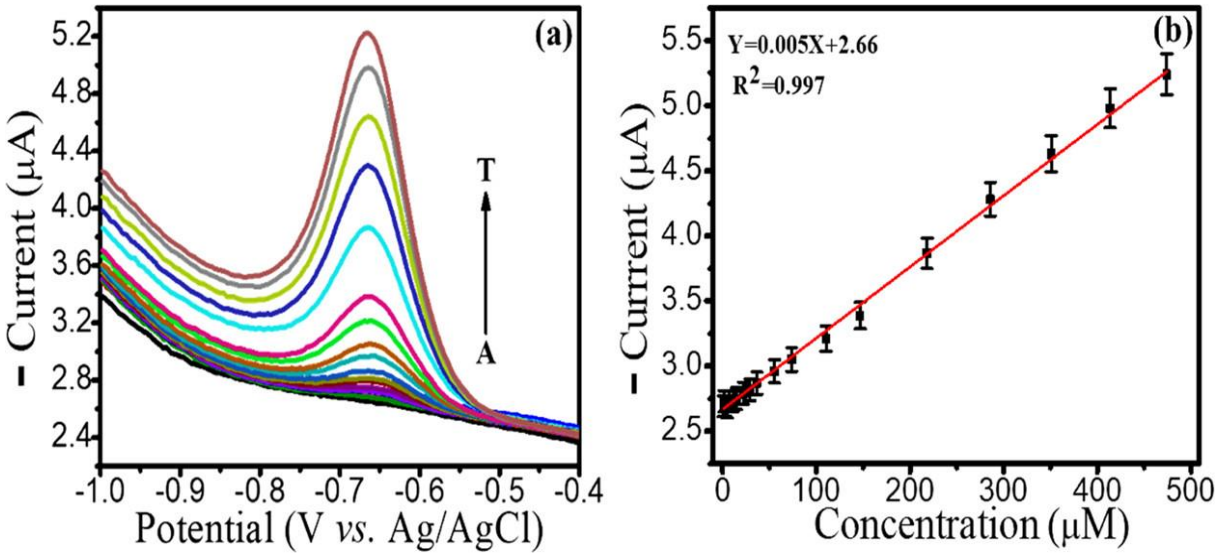

Fig. 6.3 DPV curve (a) and its calibration plot (b) of 2D carbon-modified GCE with successive addition of ROX (0 µM, then 0.76−474 µM) in deoxygenated 0.1 M PBS

Table 6.1	**Comparison of Analytical performance of ROX with other published work.**			
Technique	**LOD (nM)**	**Linearity (µM)**	**Matrix/Sample**	**Reference**
DPV	**30**	**0.05 to 490**	**phosphate buffer**	**19**
DPV	**75**	**0.1–442.6**	**phosphate buffer**	**20**
amperometric method	**22.5**	**0.035 to 1816.5**	**phosphate buffer**	**21**
DPV	**1.5** **1.8**	**0.76 to 474** **5.31 to 23.55**	**Phosphate buffer** **Blood serum**	**Our work** **Our work**

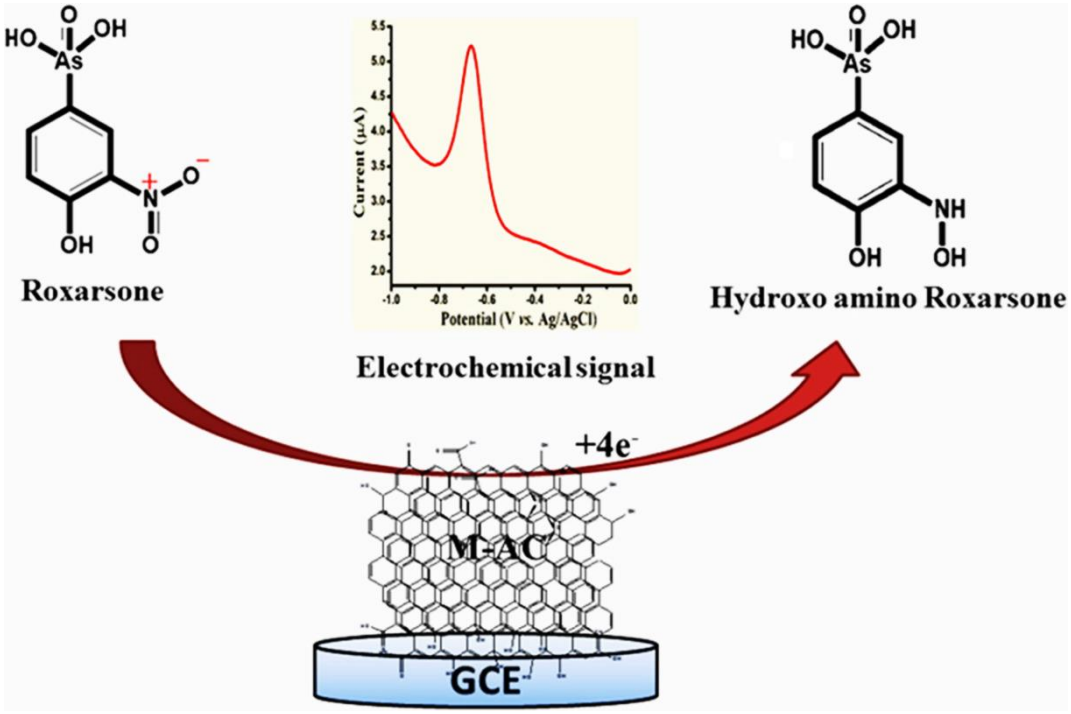

Fig. 6.4 Schematic representation of the reduction of roxarsone on the 2D carbon-modified electrode.

6.2.2.3 Validation in Real Samples

These observations lead us to perform subsequent experiments in real samples under the above-mentioned conditions. Therefore, the practical applicability of 2D carbon-modified GCE was determined in a human blood serum sample using the same DPV technique. The sample was diluted with PBS buffer in a 1:10 ratio. Then, the prepared solution was spiked with different known concentrations of ROX and analyzed using DPV under the same optimized conditions as shown in Fig. 6.5. It was evident from the figure that the cathodic current increased linearly from 5.31 to 23.55 μM. Moreover, the cathodic peak current values were plotted against the concentration of ROX to obtain a straight line with R^2 = 0.984. The developed sensor proved its efficiency for use with good sensitivity of 0.571 $\mu A \cdot \mu M^{-1} \cdot cm^{-2}$, LOQ of 5.31 μM, and LOD of 1.8 nM. Thereafter, the reduction of ROX was also validated over commercially available and disposable screen-printed carbon electrode (SPCE), which was a ready-to-use electrode

as shown in Fig.6.6. SPCE modification was carried out as discussed in the experimental section. The figure showed regular enhancement in the cathodic current peak with increasing concentration of ROX. Fig.6.6(b) shows its corresponding calibration plot having good linearity with R^2 = 0.978 with 0.0519 $\mu A \cdot \mu M^{-1} \cdot cm^{-2}$ sensitivity. Here, LOD obtained was 5.17 nM, whereas LOQ was 1.89 µM.

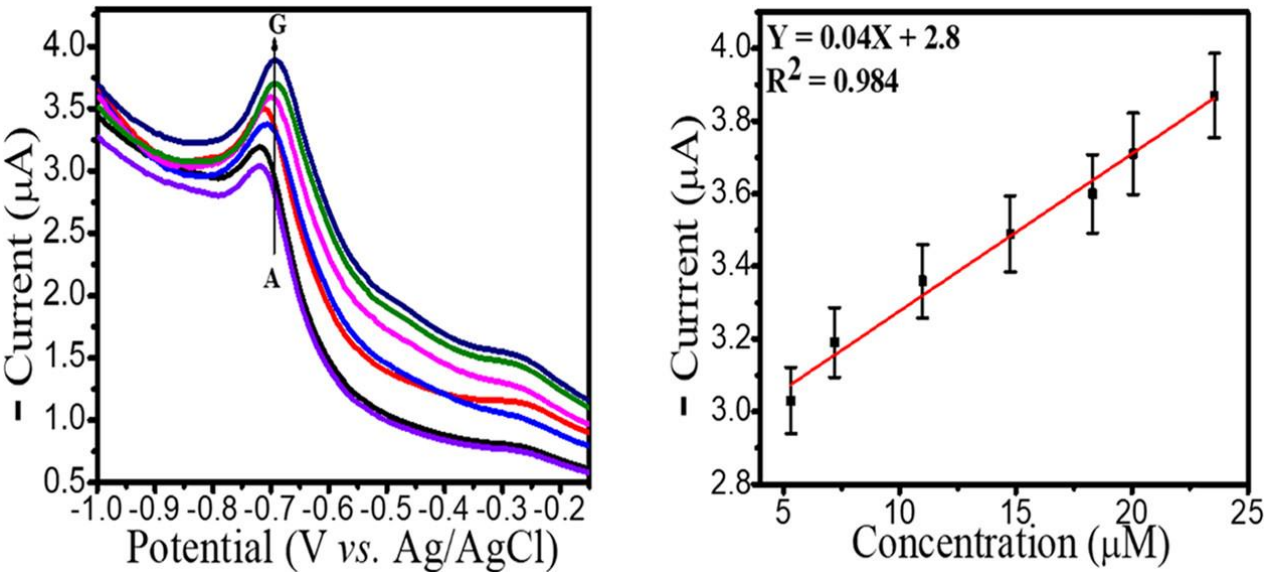

Fig.6.5 DPV curve and its calibration plot of 2D-AC-modified GCE with successive addition of ROX (5.31−23.55 µM) in deoxygenated 0.1 M PBS (pH 7.0) in human blood serum at a 50 mV s^{-1} scan rate.

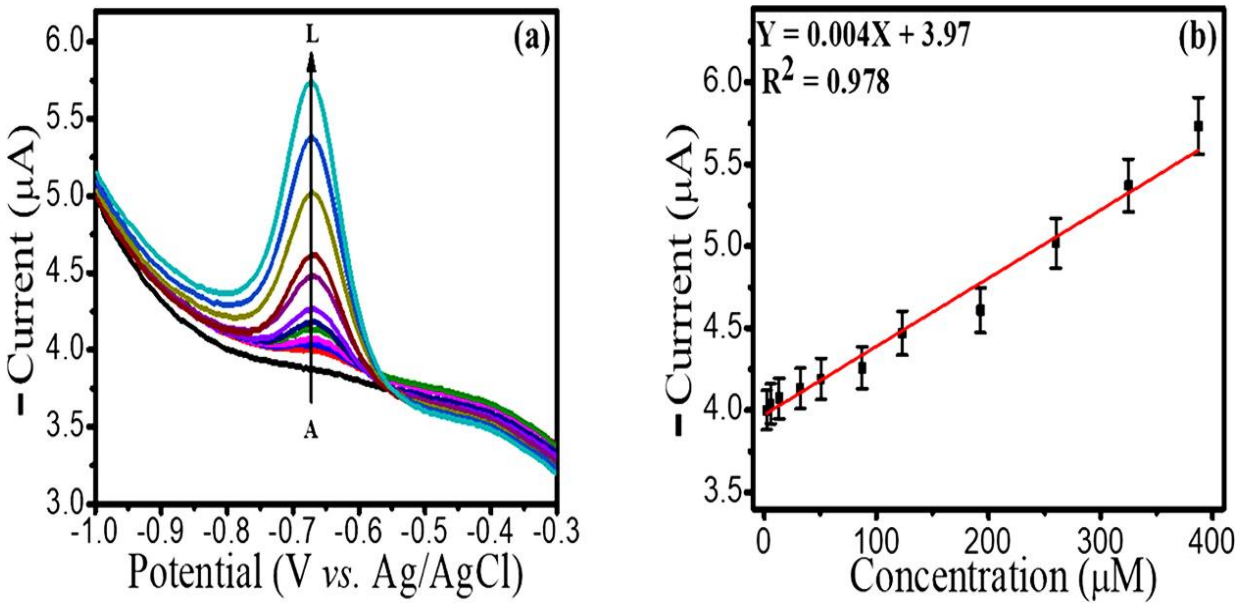

Fig.6.6 DPV curve (a) and its calibration plot (b) of M-AC-modified SPCE with successive addition of ROX (1.89−387.34 μM) in deoxygenated 0.1 M PBS (pH 7.0) at 50 mV s^{-1}.

6.2.2.4 Reproducibility and Storage Stability Test

Keeping all parameters the same, electrode modification was carried out in four sets. Then, the corresponding DPV in 0.1 M PBS with 76 μM ROX was performed, and it was found that all of the four curves almost coincided with each other, suggesting good reproducibility of the prepared sensor. Fig.6.7(a) shows up to 97% retention in the current. Further, the storage ability of the as-developed sensor was tested for 1 month. Fig. 6.7(b)

shows the DPV curve on the first day and after its thirtieth day, whereas its inset showed percentage current retention at an interval of 3 days for the next 30 days. The bar graph showed excellent stability up to 30 days with little attenuation incurrent when stored at ambient temperature. During storage, no extraordinary condition was maintained, and it was found that about 95% current was retained even after 1 month. It can be visualized from these findings that the proposed sensing platform can be safely used for a month or more than that with good accuracy for the detection of ROX.

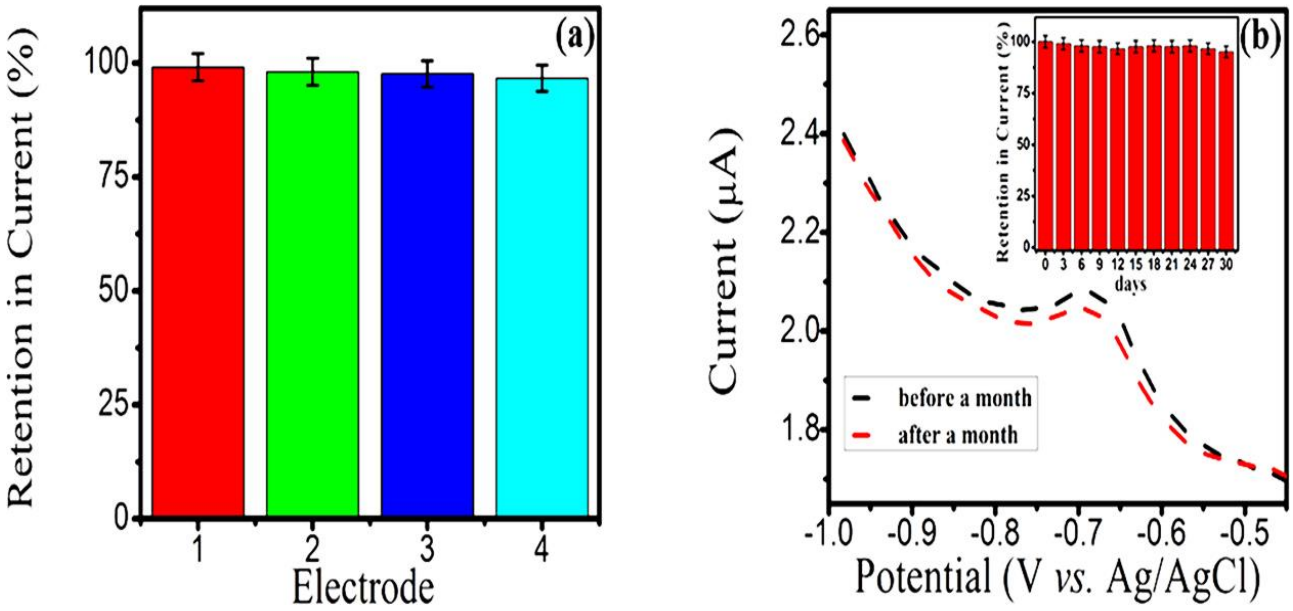

Fig. 6.7 (a) Reproducibility and (b) storage stability test of the 2D carbon-modified electrode using DPV in the presence of 76 µM ROX in 0.1 M phosphate buffer (pH 7). The inset shows % current retention in the interval of 3 days.

6.2.2.5 Study of Interference

To explore further the selectivity of 2D carbon-modified electrode toward ROX sensing, several interferents were added along with ROX, and the results were investigated in percentage change in the cathodic current in DPV in the presence of 0.1 M PBS (pH 7).

The concentration of all interferents (Na_2S, NO_2^-, NO_3^-, D-glucose, paracetamol tablet, ascorbic acid, and folic acid) was taken to be 10 times higher than that of ROX. Results shown in Fig. 6.8 depict that the 2D carbon-modified electrode was able to anti-interfere with roxarsone even with much higher concentrations of interferents in this electrochemical sensing and was fit for use in biological samples. The most probable reason for this selectivity is that AC exhibited a high adsorption capacity for ROX, which was presumably attributed to the interaction of electrostatic attraction, hydrogen bonding,

and π–π interaction between the adsorbent and the adsorbate [434]. Also, in voltammetry scans, biomolecules and drugs show no peak response or no reduction peak in the region where ROX shows reduction.

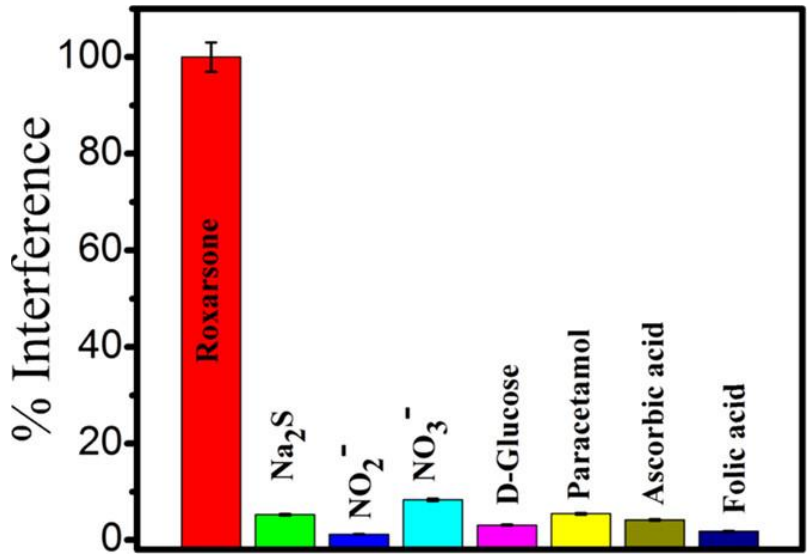

Fig.6.8 Interference study using various biological compounds toward ROX in a 10:1 ratio in 0.1 M phosphate buffer (pH 7).

6.3 Conclusions

In summary, we proposed the synthesis of meso/microporous activated carbon as a sustainable, eco-friendly, and easy-to-employee material for electrode modification and further use it for the electrochemical sensing of arsenic-based medicine ROX through DPV. The as-prepared 2D carbon was characterized using XRD, Raman and FTIR spectroscopies, TEM, and SEM. The meso/microporous nature of AC was validated using N_2 adsorption−desorption isotherms and BET analysis with a specific surface area of 194 m^2 g^{-1}. The performance of the as-synthesized 2D carbon was also validated with commercially available graphite powder for electrode modification. The superiority of 2D-AC was proved by comparing its EAS value with Gr-modified GCE and bare GCE as 0.075, 0.065, and 0.052 cm^2, respectively. 2D carbon showed excellent electrocatalytic

behaviour based on an enzyme-free sensor for the detection of the toxic drug roxarsone. Under optimum conditions, the ROX sensor is designed and developed and works well at −0.66 V (vs Ag/AgCl). Specific features of the proposed sensor include a wide linear series (0.76−474 μM) with a detection limit in the nanomolar range (1.5 nM) and good sensitivity (0.0714 $\mu A \cdot \mu M^{-1} \cdot cm^{-2}$) on glassy carbon electrode. 2D carbon-modified electrodes have been effectively applied in human blood serum samples toward the determination of ROX (LOD = 1.8 nM). They work well with screen-printed carbon electrodes (SPCEs), also showing reliable sensitivity and LOD. Results show a potential to be used as an electrochemical platform for the catalyzing ability of economically synthesized 2D carbon toward ROX (toxic arsenic-based antibiotic medicine) in real samples with a good recovery rate using DPV. The as-synthesized 2D-AC proves itself as a promising electrode material and may be apprehended in a short time. The developed sensor is validated for selectivity, storage stability, and reproducibility toward ROX. These findings recommend it as a promising method for sensing ROX electrochemically for arsenic-based chemical detection.